UNIVERSITÀ DEGLI STUDI DI PADOVA

Dipartimento di Fisica e Astronomia "Galileo Galilei"

Corso di Laurea in Fisica

Tesi di Laurea

Anomalous diffusion of critical polymers

Relatore

Prof. Fulvio Baldovin

Laureando

Sofia Marchioretto

Anno Accademico 2021/2022

Contents

Introduction

Back in 1905 Einstein published a famous paper [4] explaining the origin of the extremely irregular motion showed by small particle immersed in a liquid, named Brownian motion after Robert Brown, the botanist who first observed the phenomenon in 1827. Einstein was the first to trace back the cause of such irregularities to collisions between the particle itself and incessantly moving liquid molecules, as a result of thermal agitation. Its work describe the particle position with Gaussian statistics, as we will see in depth in chapter 2 of this thesis.
In recent years many experiments in a variety of complex fields, show a similar motion, yet with non-Gaussian statistics, arising the theoretical problem of developing suitable physical models to explain and predict such anomalous motions. In this thesis one of this models is reviewed, namely the diffusion motion of the center of mass (CM) of a polymer which has been put in contact with a chemostatted bath, allowing its size to vary. We show how this microscopic prototype, described in chapter 3, displays a complex, non-Gaussian, phenomenology through independent simulations of the process, which will be presented in chapter 4.

Ordinary Brownian motion

In this section we summarize the most important results concerning Brownian motion of a colloidal particle, introducing the mathematical framework that allows us to study and simulate this particular stochastic process.
A colloidal particle is a solid particle suspended in a liquid phase, with size between 10 nm and $1 - 10$ μm. It is small enough that its dynamic is determined by exceedingly frequent collisions with moving solvent molecules. Its position $X(t)$ in 1-dimensional space is therefore a stochastic process, whose study can be addressed in two different ways: the first one considers $p_X(x,t)$, i.e. probability density function for the position X, which satisfies a deterministic differential equation, the second one follows the evolution in time of a single realization of the process, with a stochastic differential equation.

2.1 Diffusion equation

Einstein work on Brownian motion follows the first approach and begins by considering a time interval τ, which is small compared to macroscopic observables typical time scales, but yet large enough that the motion of the particle in two consecutive time intervals can be regarded as two independent events, because of the huge number of collisions happening during τ. Probability of finding the particle in a position between x and $x + dx$ at time t, i.e. PDF of the position random variable $X(t)$, is found to satisfy the one dimensional diffusion equation [1]

$$\frac{\partial p_X(x,t)}{\partial t} = D\frac{\partial^2 p_X(x,t)}{\partial x^2} \tag{2.1}$$

where D, called *diffusion coefficient*, is defined as the mean-square displacement exhibit by the particle in time τ divided by 2τ.
Once set the initial condition $p_X(x, t = 0) = \delta(x - x_0)$, meaning the motion starts with certainty from the initial position x_0, Eq. (2.1) is solved by

$$p_X(x,t) = \frac{1}{\sqrt{2\pi}\sqrt{2Dt}} e^{-\frac{(x-x_0)^2}{4Dt}} \tag{2.2}$$

which is evidently a gaussian PDF with variance $Var[X(t)] = \langle X^2(t)\rangle - \langle X(t)\rangle^2 = 2Dt$, where $\langle X(t)\rangle$ is the expectation value for the variable $X(t)$.

[1] a brief account of Einstein work, including derivation of diffusion equation, can be found in [5].

2.2 Continuous Markov process

The second approach involves *continuous Markov process*, that is a *memoryless* stochastic process: increment in X from time t to $t+dt$ depends only on t, dt and the value x taken by X at t. In other words, knowledge of any previous state of X cannot sharpen the process *pdf* at current time. This fundamental feature, together with the requirements of continuity of X and differentiability of $X(t+dt)-X(t)$ with respect to t, dt, x, leads [6] to the Langevin equation for the process X

$$X(t+dt) = X(t) + A(X(t),t)dt + \sqrt{2D(X(t),t)}\mathcal{N}(t)\sqrt{dt} \tag{2.3}$$

where $\mathcal{N}(t) = \mathcal{N}(0,1)$ is the temporally uncorrelated unit normal random variable, with zero mean, unit variance and $\langle \mathcal{N}(t)\mathcal{N}(t')\rangle = \delta(t-t')$. $A(x,t)$ and $D(x,t)$ are smooth function that specify each process.
To study Brownian motion we specifically rely on *driftless Wiener process*, which has $A(x,t) = 0$ and $2D(x,t) = c$, with $c > 0$. Its Langevin equation reads:

$$X(t+dt) = X(t) + \mathcal{N}(t)\sqrt{c\,dt} \tag{2.4}$$

Another common form of Eq. (2.4) is:

$$\frac{dX(t)}{dt} = \sqrt{c}\Gamma(t) \tag{2.5}$$

obtained from the definition of Gaussian white noise $\Gamma(t)$[2]

$$\Gamma(t) = \lim_{dt\to 0} \mathcal{N}(0, 1/dt) = \lim_{dt\to 0} \frac{\mathcal{N}(0,1)}{dt^{1/2}}$$

We stress that Eq. (2.5) can be accounted only as a formal equation because the function $X(t)$ is not, in fact, differentiable with respect to time.

In the following lines we show that the stochastic process $X(t)$, solution of the Langevin equation with initial condition $X(0) = \delta(x - x_0) = \mathcal{N}(x_0, 0)$, is the normal variable

$$X(t) = \mathcal{N}(x_0, 2Dt). \tag{2.6}$$

To begin with we note that $X(0+dt)$ is a linear combination of two statistically independent normal variable, $X(0)$ and $\mathcal{N}(0)$, therefore it is also normal. By induction we then infer that $X(t)$ is normal for all $t > 0$.
Averaging Eq. (2.4), thanks to $\langle \mathcal{N}(t)\rangle = 0$, we obtain a differential equation for $\langle X(t)\rangle$ whose straightforward solution is $\langle X(t)\rangle = x_0$.
Next we square Eq. (2.4) and average the result, finding out:

$$X^2(t+dt) = X^2(t) + 2X(t)\mathcal{N}(t)\sqrt{c\,dt} + \mathcal{N}^2(t)\,c\,dt$$
$$\langle X^2(t+dt)\rangle = \langle X^2(t)\rangle + c\,dt \qquad \rightarrow \qquad \frac{\langle X^2(t+dt)\rangle - \langle X^2(t)\rangle}{dt} = c$$

using the relations $\langle X(t)\mathcal{N}(t)\rangle = \langle X(t)\rangle\langle \mathcal{N}(t)\rangle = 0$ and $\langle \mathcal{N}^2(t)\rangle = 1$. We have deduced a differential equation for $\langle X^2(t)\rangle$ with solution $\langle X^2(t)\rangle = c\,t$.
As a result we deduce that driftless Wiener process reproduces the exact results obtained by Einstein if we set the constant $c = 2D$.

[2] We recall that, for Normal random variables, $a + b\mathcal{N}(\mu,\sigma^2) = \mathcal{N}(a+b\mu, b^2\sigma^2)$.

2.3 Simulation and results

Markov process approach offers a simple way to simulate the process X applying Eq. (2.4) wherein dt is a fixed time interval and $\mathcal{N}(t)$ is substituted by a sample value of the unit normal random variable. The simulation algorithm basically implement this formula starting from $x(0) = 0$, updating t and $x(t)$ in consecutive dt steps until some t_{stop}. Repeating the steps for a number R of different realizations allows to collect a sample of R values from $X(t)$ for each time t, and therefore to reconstruct its PDF $p_X(x, t)$. In the next lines simulation results are reported.

In the side graph we present a view of R=3 realizations of the process, along with lines representing the expected $x_{mean} \pm \sigma_x = 0 \pm \sqrt{2Dt}$. Data were obtained with $2D = 1$, $dt/t_{stop} = 10^{-3}/6$.
Two of the major features of the motion are clearly visible: non-differentiability of the path and its great variability.

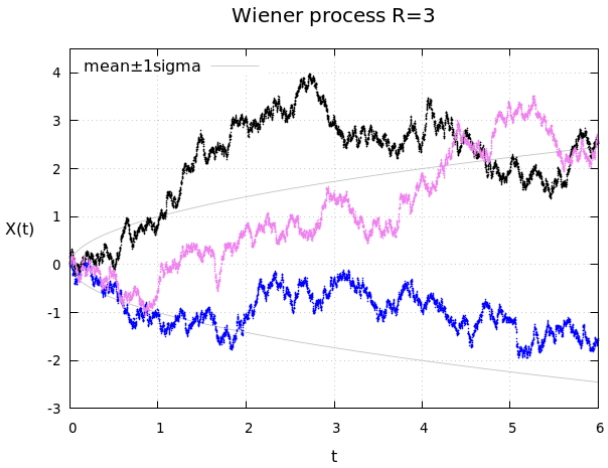

Figure 2.1: 3 realizations of Wiener process are presented, along with lines representing $x_{mean} \pm \sigma_x$. Time t is in arbitrary simulation units, whereas space X is defined in units of $\sqrt{2Dt}$.

Next we analyze first and second moment of the variable $X(t)$, computing average and variance over R values taken by X at each time t. The following plots show evolution in time of the two moments for different values of R, versus the expected values computed from Eq. (2.6) where $x_0 = 0$, $2D = 1$. Time t is in arbitrary simulation units, whereas space X is defined in units of $\sqrt{2Dt}$.

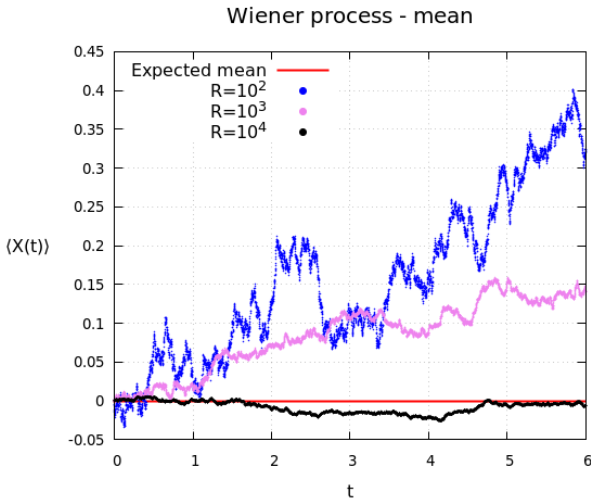

Figure 2.2: Time evolution of the mean of $X(t)$ computed over R realization of the process.

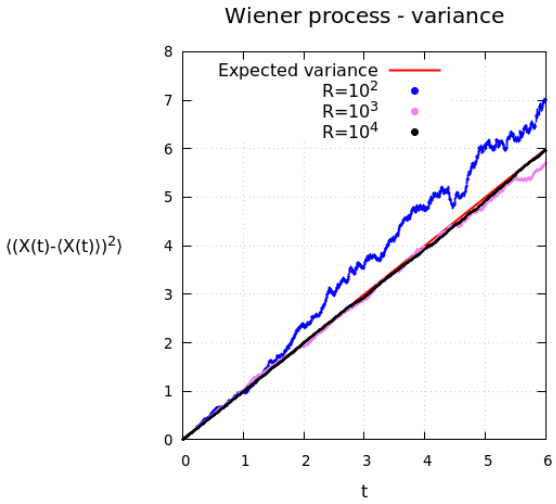

Figure 2.3: Time evolution of the mean of $X(t)$ computed over R realization of the process.

Obviously, the plots show that data agreement with the model (red line in plot) grows with R. In conclusion, the expected behaviour is confirmed.

At each simulation time t, the $X(t)$ expected PDF can be compared with an histogram of the sample values obtained by R simulations.

In the side graph we present histograms for X at time $t/dt = 3$ and $t/dt = 50$, along with the expected PDF computed from Eq. (2.6). Data were obtained with $2D = 1$, $dt/t_{stop} = 10^{-3}/6$, $R = 10^4$.
The effect of Brownian diffusion is evident: the PDF of the particle position spreads through space remaining Gaussian and centered in the origin. Agreement between data and expected values is satisfactory.

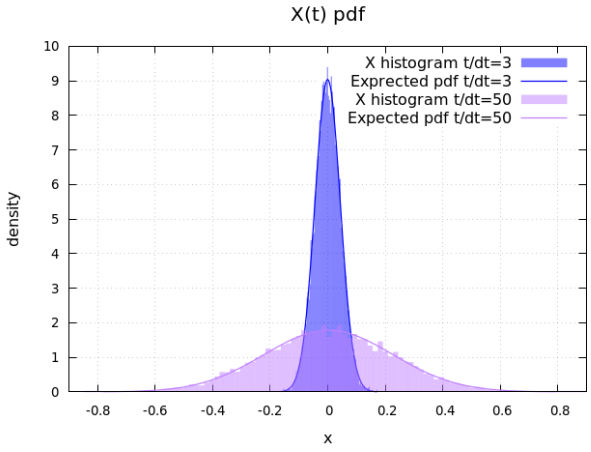

Figure 2.4: Histograms for X at time $t/dt = 3$ and $t/dt = 50$, along with the expected pdf. X is in units of $\sqrt{2Dt}$.

Polymers

3.1 Introduction

Polymers are complex molecules playing a fundamental role in biology as well as in biophysics and modern physics. Homopolymers are made up by a large number of identical building blocks, i.e. monomers, that can be organized in different topological structures. We will only consider polymers arranged in a linear chain of monomers, in which every one of them can make up to two bonds.
The Rouse model is one of the simplest model to derive dynamical properties of polymer immersed in a liquid because it neglects the hydrodynamic effect induced by the moving fluid to the polymer: the only interaction between consecutive monomers is then modeled with an elastic attractive potential. We write 1-dimensional equation of motion for the i-th monomer, with position X_i, out of n total monomers in the chain, adapting the 3-dimensional equations found in [1]

$$\begin{aligned}
\frac{dX_1}{dt} &= -\omega\left(X_1 - X_2\right) + f_{x,1}(t) \\
\frac{dX_i}{dt} &= -\omega\left(X_i - X_{i+1} + X_i - X_{i-1}\right) + f_{x,i}(t) \\
&= -\omega\left(2X_i - X_{i+1} - X_{i-1}\right) + f_{x,i}(t) \qquad \text{if } 1 < i < n,\ i \in \mathbb{N} \\
\frac{dX_n}{dt} &= -\omega\left(X_n - X_{n-1}\right) + f_{x,n}(t)
\end{aligned} \tag{3.7}$$

where ω denotes a coefficient depending on temperature, length of the bond and drag coefficient of the single monomer, while $f_{x,i}(t) = \sqrt{2D_0}\Gamma(t)$ is the x-component stochastic force exerted on the i-th monomer, with diffusion coefficient D_0.
Equations (3.7) allow to derive the center of mass equation of motion

$$\frac{dX_{CM}}{dt} = \frac{1}{n}\sum_{i=1}^{n} f_{x,i}(t) \qquad \rightarrow \qquad X_{CM}(t) = X_{CM}(0) + \int_0^t \frac{1}{n}\sum_{i=1}^{n} f_{x,i}(t')dt' \tag{3.8}$$

Using then the relations $\langle f_{x,i}(t) f_{x,j}(t')\rangle = 2D_0\delta_{i,j}\delta(t-t')$ and $\langle X_{CM}(t) - X_{CM}(0)\rangle = 0$ it can be obtained

$$Var\left[X_{CM}(t) - X_{CM}(0)\right] = \left\langle \left(X_{CM}(t) - X_{CM}(0)\right)^2 \right\rangle = \frac{2D_0}{n}t \tag{3.9}$$

The center of mass of a polymer made by n monomers is subject to standard Brownian motion with a diffusion coefficient $D_{CM} = D_0/n$.

3.2 Birth death process

When the polymer is in contact with a chemostatted bath, that is a liquid containing its monomers, polymerization or depolymerization can occur, through respectively attachment or detachment of a monomer to the chain, varying its size. We briefly overview *birth-death process* as a suitable mathematical model describing this physical situation.
The discrete polymer size $N(t)$ is a Markov Process that, during the time interval $(t, t+\Delta t)$, starting from the value n, can increase by one with probability $\lambda\Delta t + o(\Delta t)$, or decrease by one with probability $\mu\Delta t + o(\Delta t)$. λ and μ are respectively called birth and death rates and we consider them as being independent of n. When N takes on the minimum value, $n = n_{min}$, which can vary depending on the model, the decreasing probability is zero.
Defining $P_N(n,t)$ the probability of the event $N = n$ at time t, equations for evolution of such probabilities, namely Master equations, can be deduced applying conservation of total probability. In particular the state $N(t+\Delta t) = n$ can be achieved by either one of the following situations: $N(t) = n+1$ and a death occurs during Δt, $N(t) = n$ and neither a death nor a birth happen during Δt or $N(t) = n-1$ and a birth occurs in Δt:

$$\begin{cases} P_N(n, t+\Delta t) = P_N(n+1,t)\mu\Delta t + P_N(n,t)(1-\lambda-\mu)\Delta t \\ \qquad\qquad + P_N(n-1,t)\lambda\Delta t + o(\Delta t) \qquad \text{if } n \geq n_{min} \\ P_N(n_{min}, t+\Delta t) = P_N(n_{min}+1,t)\mu\Delta t + P_N(n_{min},t)(1-\lambda\Delta t) + o(\Delta t) \end{cases} \tag{3.10}$$

taking the limit $\Delta t \to 0$

$$\begin{cases} \frac{dP_N(n,t)}{dt} = \mu P_N(n+1,t) - (\lambda+\mu)P_N(n,t) + \lambda P_N(n-1,t) \quad \text{if } n \geq n_{min} \\ \frac{dP_N(n_{min},t)}{dt} = \mu P_N(n_{min}+1,t) - \lambda P_N(n_{min},t) \end{cases} \tag{3.11}$$

We now look for a stationary solution $P_N^*(n)$ imposing the condition $\frac{dP_N^*(n)}{dt} = 0\ \forall n,t$ in Eq. (3.11). Defining the growth factor $g = \lambda/\mu$ we obtain

$$\begin{cases} P_N^*(n+1) = (1+g)P_N^*(n) - gP_N^*(n-1) \\ P_N^*(n_{min}+1) = gP_N^*(n_{min}) \end{cases} \tag{3.12}$$

Using the first equation we note that, if $P_N^*(n)/P_N^*(n-1) = g$, then also the relation $P_N^*(n+1)/P_N^*(n) = g$ stands. Since $P_N^*(n_{min}+1)/P_N^*(n_{min}) = g$ we conclude by induction that

$$P_N^*(n+1)/P_N^*(n) = g\ \ \forall n \qquad \to \qquad P_N^*(n) = g^{n-n_{min}}P_N^*(n_{min}) \tag{3.13}$$

Normalizing probabilities leads to:

$$\sum_{n=n_{min}}^{+\infty} P_N^*(n) = 1 \qquad \overset{(3.13)}{\to} \qquad P_N^*(n_{min}) = \frac{1}{\sum_{n=n_{min}}^{+\infty} g^{n-n_{min}}} = 1-g \quad \text{if } g<1$$

Finally the solution is then

$$\begin{cases} P_N^*(n) = g^{n-n_{min}}(1-g) & \text{if } n \geq n_{min},\ n \in \mathbb{N} \\ P_N^*(n) = 0 & \text{otherwise} \end{cases} \tag{3.14}$$

A full, time-dependent solution of the master equation (3.11) can be found in [7]. From that, it is possible to calculate the auto-correlation coefficient $N(t)$, reported in the following:

$$\rho(t) = \frac{\langle N(t)N(0)\rangle - (\langle N\rangle)^2}{\langle N^2\rangle - (\langle N\rangle)^2} \approx e^{-t/\tau} \qquad \tau = \frac{1+g}{(1-g)^2\mu} \tag{3.15}$$

3.3 Critical polymers

Applying Eq. (3.14) we calculate expectation value for the variable N, at equilibrium, and the corresponding expected variance:

$$\langle n \rangle = \sum_{n=n_{min}}^{+\infty} n P_N^*(n) = \sum_{n=n_{min}}^{+\infty} n g^{n-n_{min}}(1-g) = \frac{g}{1-g} + n_{min} \tag{3.16}$$

$$\left\langle (n - \langle n \rangle)^2 \right\rangle = \sum_{n=n_{min}}^{+\infty} (n-\langle n \rangle)^2 P_N^*(n) = \sum_{n=n_{min}}^{+\infty} \left(n - n_{min} - \frac{g}{1-g} \right)^2 g^{n-n_{min}}(1-g) = \frac{g(4g+1)}{(1-g)^2} \tag{3.17}$$

It can be clearly observed that $\langle n \rangle \to +\infty$ and $\left\langle (n - \langle n \rangle)^2 \right\rangle \to +\infty$ when $g \to 1^-$. The divergence in the polymer size proves the presence of the critical point $g = 1$, which divides a thermodynamic region ($g < 1$) where the polymer has a finite size and is in a dilute phase, from another thermodynamic region ($g > 1$) where the polymer is characterized by infinite size and is called in a dense phase, because, when placed in a monomer bath, it tends to polymerize and occupy all the available volume (e.g. [2]).
For a better understanding of the physical context, in the following lines we link the growth factor g to concentration of monomers in the bath, and specifically to chemical potential μ perceived by the polymer.
Dynamic of varying-size polymers is effectively studied within the grand canonical ensemble, thanks to grand canonical partition function, which, following our model, depends only on chemical potential, or equivalently on monomer fugacity $z = e^{\beta\mu} = e^{\mu/k_B T}$. As criticality is approached it reads ([2], [3])

$$Z_{gc}(z) = \sum_n \left(\frac{z}{z_c} \right)^n n^{\gamma-1} \tag{3.18}$$

where z_c is the inverse of the connective constant μ_c, related to the typical number of bonds established by a single monomer, while universal entropic exponent γ is linked to the space dimension of the polymer lattice, to its underlying topology and to equilibrium phase. We will consider $\gamma = 1$ in the following, according to the mean field limit.
Consequently, equilibrium probabilities of N taking a specific value n can be written:

$$P_N^*(n) = \frac{(z/z_c)^n}{Z_{gc}(z)} \tag{3.19}$$

Applying Eq. (3.13) we conclude

$$g = \frac{P_N^*(n+1)}{P_N^*(n)} = \frac{(z/z_c)^{n+1}}{Z_{gc}(z)} \frac{Z_{gc}(z)}{(z/z_c)^n} = \frac{z}{z_c}$$

We therefore understand that criticality arises when $z \to z_c^-$.

Anomalous diffusion

4.1 Theoretical framework

As we have seen above, the center of mass of a polymer diffuses with a diffusion coefficient D_{CM} which depends on its size n. When in contact with a chemostatted bath the size n varies with time, with a minimum n_{min}. Setting $n_{min} = 3$, as we do in the following, allows the minimum size polymer to independently attach or detach a monomer at both ends of the chain with size-independent birth and death rates λ, μ. As a result of polymerization or depolymerization even D_{CM} undergoes variations throughout the motion. When n fluctuations are limited, the anomalous effects on diffusion are hard to detect but when, instead, the system is close to its critical point, n fluctuations diverge, as we have seen in Eq. (3.17), resulting in great variability of D_{CM}. The parameter controlling the divergence is g: as it approaches the value 1^- criticality arises. As an outcome, the motion of the polymer CM is Brownian yet non Gaussian. In the next lines we outline theoretical results explaining the anomalous behaviour, all of which have been originally developed in [8] and in references therein.
Considering the motion starting from the origin, $X_{CM}(t = 0) = 0$, the diffusion equation reads

$$\frac{\partial p_{X_{CM}}(x, t|\,[n(t)])}{\partial t} = \frac{D_0}{n(t)} \frac{\partial^2 p_{X_{CM}}(x, t|\,[n(t)])}{\partial x^2} \tag{4.20}$$

depending on the full evolution of N stochastic process between 0 and t, denoted with $[n(t)] = \{n(t') \in \mathbb{N} | 0 \leq t' \leq t\}$. Defining the path random variable s, which corresponds to the realization of the process:

$$S(t) = \int_0^t 2D_{CM}(N(t'))dt' \tag{4.21}$$

Eq. (4.20) returns to be an ordinary diffusion equation

$$\frac{\partial p_{X_{CM}}(x, s)}{\partial s} = \frac{\partial^2 p_{X_{CM}}(x, s)}{\partial x^2} \tag{4.22}$$

Therefore, with respect to s, the solution is a normal probability function with variance s

$$p_{X_{CM}}(x, s) = \frac{1}{\sqrt{2\pi s}} e^{-\frac{x^2}{2s}} \tag{4.23}$$

Returning to t variable, $X_{CM}(t)$ PDF for a process starting from $N(0) = n_0$ and $X_{CM}(0) = 0$ is then expressed in an integral form

$$p_{X_{CM}}(x, t|n_0) = \int_0^\infty \frac{e^{-\frac{x^2}{2s}}}{\sqrt{2\pi s}} p_S(s, t|n_0) ds \tag{4.24}$$

where $p_S(s, t|n_0)$ is $S(t)$ PDF. Equation (4.24) explicitly marks non-Gaussianity of the CM motion: when $p_S(s, t|n_0)$ is not a delta function, indeed, $p_{X_{CM}}$ is the continuous sum of gaussian PDFs with different variances s, resulting in a leptokurtic distribution with fat tails.

4.2 Simulation algorithm

In the present sections we explain the simulation procedure that has been extensively applied to study the CM position stochastic process. The algorithm adds the simulation of birth death process for the polymer size n on top of the algorithm for standard Brownian diffusion. The routine is summarized in what follows:

1. Birth and death rates are specified: $\mu = 1$ and $\lambda = g\mu$, where g is set by user: the closer it gets to 1, the higher critical effects will be.
2. As we demonstrate in appendix 6.1.1 the average time interval between one birth/death event and the next, called departure time, is $T = 1/(\lambda + \mu)$. The updating time interval, dt, is therefore set to $dt = 0.1/(\lambda+\mu)$. Next τ is computed from (3.15) and t_{stop} is declared in units of τ. We see that when g is closer to 1, for the time sampling to be effective, dt becomes smaller and τ diverges to $+\infty$: in this way computational time explodes.
3. Simulations starts at time $t = 0$ when size n ($n \geq 3$) is initialised in two manner depending on the need: to a fixed starting value n_0 decided by user, or it is randomly generated according to its equilibrium probability distribution, as will be explained in appendix 6.2.
4. Departure time is then randomly generated, according to his exponential PDF, using Gillespie algorithm provided in appendix 6.1.1. t evolves in dt steps: while $t <$ departure time, standard algorithm for diffusion updates the CM position x at each step with diffusion coefficient $D = D_0/n$. When t becomes bigger than departure time, a birth/death event has happened: Gillespie algorithm randomly generate if the event is a "birth" or a "death" and n is accordingly increased or decreased by 1. D_{CM} is therefore updated with the new size n.
5. The routine described in 4. is repeated updating t, x every dt steps and n every time a new departure time is reached.
6. The whole procedure starting from point (3) is replicated for the desired number of realizations R.

4.3 Simulation results

First we look at the behaviour of the variable n when the simulations starts from a fixed initial state n_0, while $g = 0.95$. We provide analysis of data through the following plot.

In the side graph, average of n, computed over $R = 2{\cdot}10^4$ realizations, is plotted versus rescaled time t/τ. We remind that τ plays the role of a "decorrelation time", as apparent from Eq. (3.15). It is visible that the asymptotic value corresponds to expected value for n, computed in (3.16).

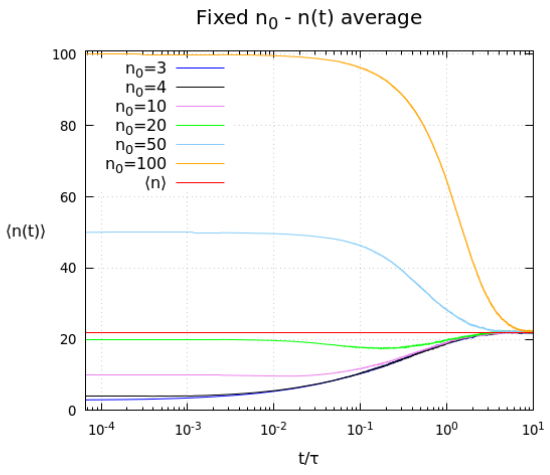

Figure 4.5: Average of n, computed over $R = 2{\cdot}10^4$ realizations, versus $time/\tau$, is plotted (g=0.95).

As expected, when initial conditions are out of equilibrium, size tends asymptotically in time to average size $\langle n \rangle = \frac{g}{1-g} + n_{min}\big|_{g=0.95} = 22$. Obviously, the further n_0 is from $\langle n \rangle$, the longer the process takes to restore equilibrium size.

Next we analyze the CM position stochastic process via its variance. Defining $P_N(n,t|n_0)$ as the probability for the size to be n at time t, starting from size n_0 at time $t = 0$, in [8] the coming result for variance of processes starting from size n_0 is derived[3]:

$$\left\langle (X_{CM}(t) - X_{CM}(0))^2 \, |n_0 \right\rangle = Var\left[X_{CM}(t)|n_0\right] = \langle S(t)|n_0\rangle = \sum_{n=3}^{\infty} \frac{2D_0}{n} \int_0^t P_N(n,t'|n_0)dt' \tag{4.25}$$

where we have used that $X_{CM}(0) = 0$ and $\langle X_{CM}(t)\rangle = 0 \ \forall t$. Therefore variance is not, in general, linear in t, as it it for ordinary Brownian diffusion. Linearity is reestabilished if $P_N(n,t|n_0) \approx P_N^*(n)$, in which case:

$$Var\left[X_{CM}(t)|n_0\right] = 2\sum_{n=3}^{\infty} \frac{D_0}{n} P_N^*(n)t = 2D_{av}t \qquad \text{with } D_{av} = \sum_{n=3}^{\infty} \frac{D_0}{n} P_N^*(n) \tag{4.26}$$

This condition is verified for fixed initial size and large time $t \gg \tau$ or for equilibrium initial condition, $\forall t$.
We display time evolution of variance in the following graph, where $Var[X(t)]/2t$ is plotted against t/τ. Processes start either from fixed initial size n_0 or from equilibrium initial condition (i.e. Equilibrium i.c.). Data are obtained for $g = 0.95$ and $R = 5 \cdot 10^4$.

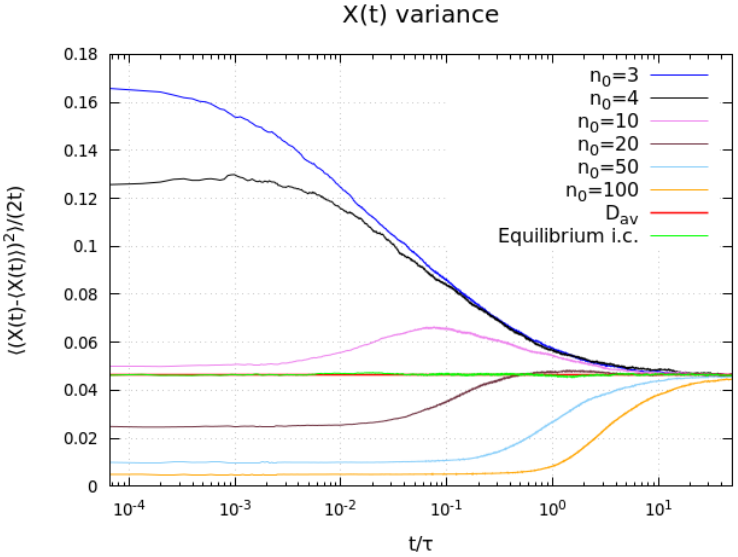

Figure 4.6: $Var[X(t)]/2t$ is plotted against t/τ, for different initial condition. $g = 0.95$ and $R = 10^5$.

The process with equilibrium initial conditions confirms the expected linear diffusion, whereas fixed initial size processes show a variety of non-linear behaviour: for example the ones with $n_0 \gg \langle n \rangle$ present superdiffusion, visible from superlinearity of variance with respect to t. This happens because n is decreasing towards $\langle n \rangle$ and diffusion coefficient is consequently increasing. On the contrary, processes with $n_0 \ll \langle n \rangle$ present subdiffusion and sublinearity of variance with

[3]Note that, here and in the following, we have adapted results from a 3-dimensional motion, as the one studied in [8], to 1-dimensional motion, as the one simulated in this thesis.

respect to t.
However, no matter what initial size is, Brownian diffusion is reached for $t \gg \tau$.

Hereafter we evaluate non-Gaussian anomalies of the random variable X_{CM} through the study of its kurtosis:

$$\kappa_X = \frac{\left\langle (X_{CM}(t) - \langle X_{CM}(t) \rangle)^4 \right\rangle}{\left(\left\langle (X_{CM}(t) - \langle X_{CM}(t) \rangle)^2 \right\rangle \right)^2} \tag{4.27}$$

We recall that for gaussian random variable $\kappa = 3$, so excess kurtosis is defined as $\kappa - 3$. We summarize theoretical results obtained in [8] to compare them with simulation data.
When initial size n_0 is specified, time evolution of kurtosis starts from $\kappa_X(t = 0^+|n_0) = 3$ signaling initial gaussian behaviour. As n PDF spreads, κ increases until a maximum is reached, then decreases, returning asymptotically to $\kappa_X(t \gg \tau|n_0) \approx 3$.
When instead, initial size is distributed according with equilibrium probability $P_N^*(n_0)$, initial kurtosis is found to be greater than 3, then tending towards this value as t increases.
This behaviour is confirmed by simulation data, presented in the following figure, where $\kappa(t) - 3$ is plotted against t/τ for different initial conditions: fixed initial size n_0 or equilibrium i.c. Data were obtained with $g = 0.95$ and $R = 10^5$.

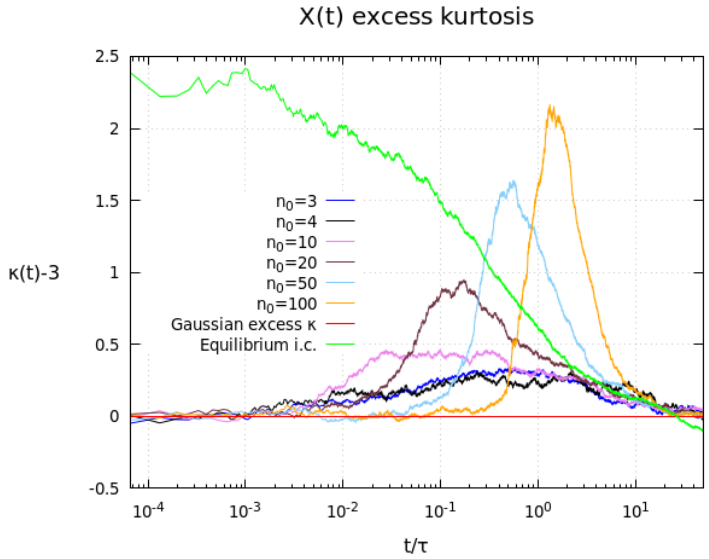

Figure 4.7: $\kappa(t)$ is plotted against t/τ for different initial conditions: fixed initial size n_0 or equilibrium i.c. g=0.95.

In particular, $\kappa_X(t = 0^+)$ diverges to ∞ when $g \to 1^-$. To show dependence of κ on g we present its time evolution for different g value. Data sets have been simulated with $R = 10^5$.
We recall that simulations with higher g have lower dt, consequently data sets plotted in the following graph starts from different points in time.

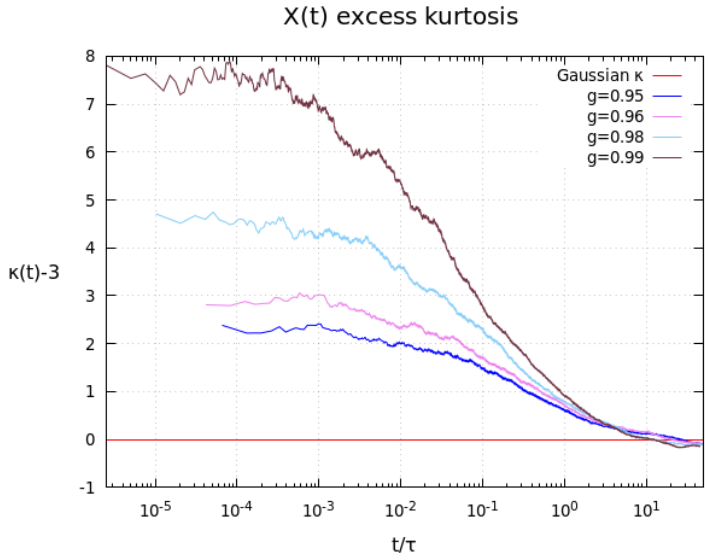

Figure 4.8: κ time evolution for different growth factors g and equilibrium initial conditions.

From the figure, it can be clearly observed that data set with higher g, corresponding to closer to criticality polymers, present greater initial kurtosis.

In the next graphs, we compare two X_{CM} histograms, computed over $R = 10^4$ realizations with $g = 0.95$ of the anomalous process, for different time t, along with corresponding Gaussian PDF.

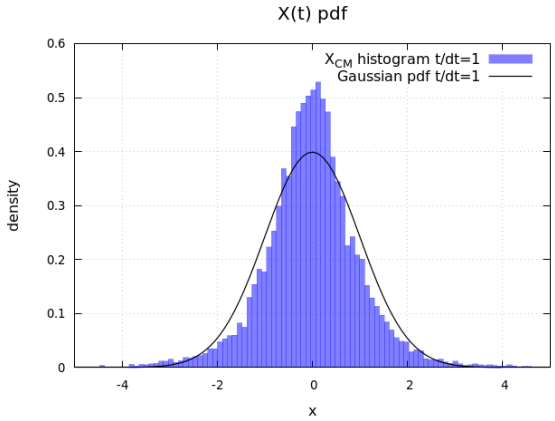

Figure 4.9: X_{CM} histogram, computed over $R = 10^4$ realizations of the anomalous process (g=0.95), for $t/dt = 1$. X is in units of $\sqrt{2Dt}$.

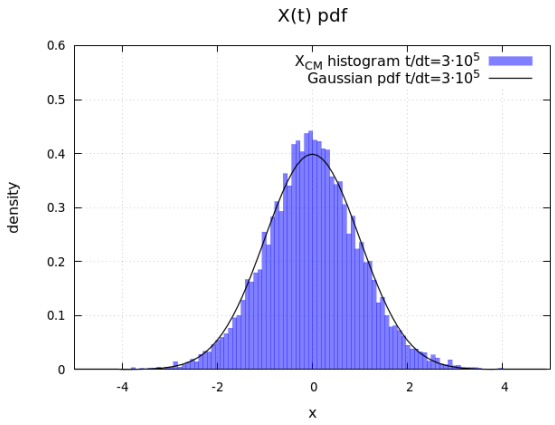

Figure 4.10: X_{CM} histogram, computed over $R = 10^4$ realizations of the anomalous process (g=0.95), for $t/dt = 3 \cdot 10^5$. X is in units of $\sqrt{2Dt}$.

The anomalous effect is evident: X_{CM} PDF for initial time is clearly non Gaussian, tending towards normal PDF as time grows.

Conclusions and future perspective

5.4 External gravitational field

In this section we briefly tackle a new physical situation of an external field acting on the diffusing polymer, such as a gravitational field positively oriented in the direction of motion. The Langevin equation for particle velocity V_x will include this new term

$$m\frac{dV_x(t)}{dt} = -\gamma V(t) + \sqrt{c}\Gamma(t) + mg \tag{5.28}$$

where γ and m are respectively the polymer drag coefficient and mass. Setting the overdamped condition $dV_x(t)/dt = 0$ and $c = 2D\gamma^2$ leads to the analogous of Eq. (2.4) and (2.5)

$$\frac{dX(t)}{dt} = V_x(t) = \sqrt{2D}\Gamma(t) + \frac{m}{\gamma}g \tag{5.29}$$

$$X(t+dt) = X(t) + \sqrt{2D}\mathcal{N}(t)(dt)^{1/2} + \frac{m}{\gamma}g\,dt \tag{5.30}$$

Carrying out the same procedure as the one shown in section 2.2 we can solve the Langevin equation under initial condition $X(t=0) = 0$. First we note that $X(t)$ is the sum of a normal random variables and a deterministic coefficient, then $X(t)$ is normal $\forall t$. Then averaging Eq. (5.30) we find

$$\langle X(t)\rangle = \frac{m}{\gamma}gt \tag{5.31}$$

understanding that in an overdamped situation gravity induces a constant velocity drift. Next we square and average Eq. (5.30), neglecting $o(dt)$, to find:

$$\begin{aligned}\left\langle X^2(t+dt)\right\rangle &= \left\langle X^2(t)\right\rangle + 2Ddt + 2\frac{m}{\gamma}g\left\langle X(t)\right\rangle dt \\ \left\langle X^2(t)\right\rangle &= 2Dt + \left(\frac{m}{\gamma}g\right)^2 t^2\end{aligned} \tag{5.32}$$

$X(t)$ is a normal random variable with quadratic variance with respect to time.

When instead the size n of the polymer can vary D, γ and m depend parametrically on n. Exploiting the well-known Einstein relation

$$\gamma D = k_B T \tag{5.33}$$

and treating $k_B T$ as a constant we derive

$$D = \frac{D_0}{n} \qquad \gamma = \frac{k_B T}{D_0}n \qquad m = m_0 n \tag{5.34}$$

where we call D_0 and m_0 respectively the diffusion coefficient and the mass of a single monomer. The Langevin equations (5.29) (5.30) then become

$$\begin{aligned} \frac{dX(t)}{dt} &= \sqrt{\frac{2D_0}{n(t)}}\Gamma(t) + \frac{D_0 m_0}{k_B T} g \\ X(t+dt) &= X(t) + \sqrt{\frac{2D_0}{n(t)}}\mathcal{N}(t)(dt)^{1/2} + \frac{D_0 m_0}{k_B T} g\, dt \end{aligned} \tag{5.35}$$

We see that, because of Eq. (5.34), the gravitational term does not depend on n.
The situation becomes more complex considering

$$D = \frac{D_0}{n^\alpha} \tag{5.36}$$

Within the Rouse model we have considered $\alpha = 1$, however other polymer models set $\alpha \neq 1$, in which case the Langevin equation reads:

$$X(t+dt) = X(t) + \sqrt{\frac{2D_0}{n(t)}}\mathcal{N}(t)(dt)^{1/2} + \frac{D_0 m_0}{k_B T}\left(n(t)\right)^{1-\alpha} g\, dt \tag{5.37}$$

where the subordinator process impacts both the diffusion process and the gravitational motion.

5.5 Conclusions

In this thesis we have reviewed the microscopical model of the motion of a chemostatted polymer center of mass as a Brownian, yet non-Gaussian, diffusion. We have conducted numerical simulations starting from two different initial scenarios: fixed polymer size or randomly generated polymer size according to equilibrium probability. We have displayed such an anomalous behaviour in terms of non linearity of variance with respect to time, as well as in terms of deviation of kurtosis from gaussian value of 3.
We have then begin the theoretical treatment of the relatively new physical situation of a diffusing chemostatted polymer which is subjected to sedimentation because of a gravity field. Further theoretical and numerical developments towards a complete understanding of this condition would be very interesting.

Appendix

6.1 Gillespie algorithm

In this section we describe Gillespie algorithm, which has been employed in birth death process simulation. Using the already introduced notation we denote with λ the birth rate and with μ the death rate.

6.1.1 Distribution of departure time

We derive departure time PDF by first recalling that probability $p_d(dt)$ that the system starting from size n will change its state in an infinitesimal time interval dt is the sum of probabilities of birth occurrence and death occurrence in the same time interval. From definition of birth and death rates (independent of n):

$$p_d(dt) = (\lambda + \mu)dt \tag{6.38}$$

Consequently, since the process is Markovian, i.e. memoryless, probability $p_d^*(t + dt)$ that the system does not change state during the interval $t + dt$ is:

$$p_d^*(t + dt) = p_d^*(t)p_d^*(dt) = p_d^*(t)(1 - (\lambda + \mu))dt \qquad \rightarrow \qquad \frac{dp_d^*(t)}{dt} = -p_d^*(t)(\lambda + \mu) \tag{6.39}$$

concluding $p_d^*(t) = e^{-(\lambda+\mu)t}$.
Probability of departure time T being exactly t is the compound probability that no jump happens until t, and a jump occurs in $(t, t + dt)$. Its PDF is therefore exponential:

$$p_T(t) = (\lambda + \mu)e^{-(\lambda+\mu)t} \tag{6.40}$$

Average departure time is

$$\langle T \rangle = \int_0^\infty t\, p_T(t)dt = \frac{1}{\lambda + \mu} \tag{6.41}$$

To randomly generate a value for T, according to its exponential PDF, the following relation can be employed:

$$T = \frac{1}{\lambda + \mu} ln\left(\frac{1}{u}\right) \tag{6.42}$$

where u is a sample from uniform random variable in $(0, 1)$.

6.1.2 Event selection

Given that a particular event has happened, probabilities for it to a birth or a death are respectively:

$$P(b|\text{an event occurs}) = \tfrac{\lambda}{\lambda+\mu} \qquad\qquad P(d|\text{an event occurs}) = \tfrac{\mu}{\lambda+\mu}$$

The simulation randomly generates u from uniform random variable in $(0, 1)$. Then birth is selected if $u < \lambda/(\lambda + \mu)$, otherwise death is selected.

6.2 Algorithm for exponential PMF sampling

At equilibrium conditions, starting size of the polymer is a random sample from the PMF (i.e. probability mass function)

$$P_N(n) = g^n(g-1) \qquad g < 1 \tag{6.43}$$

A basic algorithm has been employed to generate a random value n according to this probability function:

1. a sample u from uniform random variable between 0 and 1 is generated
2. in a loop cumulative probability C is computed: starting from $i = 0$, $C = 0$, at each iteration i increases by 1 and $P_N(i)$ adds to the previous C. The loop ends when $C > u$.
3. the final sample n is set equal to $i-1$, the last natural number for which the loop condition was verified. Then the actual size of the polymer will be $n + n_{min}$.

We attach on the side a graph proving the correct functioning of the algorithm. It shows an histogram of the computed sample values for $g = 0.95$, versus the corresponding expected PMF (6.43), which has been plot as continue line for better graphic results.

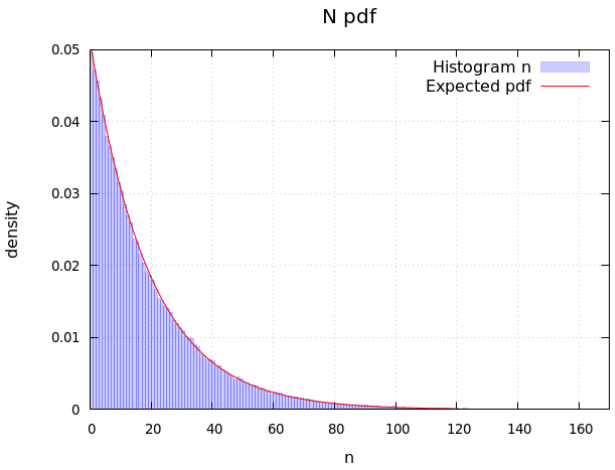

Figure 6.11: Histogram of the computed sample values for $g = 0.95$, versus the corresponding expected PMF.

Bibliography

[1] W. J. Briels. Theory of polymer dynamics, 1998.

[2] P. de Gennes. *Scaling concepts in polymer physics*. Cornell Univ. Pr., 1979.

[3] P. G. de Gennes. Exponents for the excluded volume problem as derived by the Wilson method. *Phys. Lett. A*, 38:339–340, 1972.

[4] Albert Einstein. On the motion of small particles suspended in liquids at rest required by the molecular-kinetic theory of heat. *Annalen der Physik*, 17, 1905.

[5] C. W. Gardiner. *Handbook of stochastic methods for physics, chemistry and the natural sciences*, volume 13 of *Springer Series in Synergetics*. Springer-Verlag, Berlin, third edition, 2004.

[6] Daniel T. Gillespie. The mathematics of brownian motion and johnson noise. *American Journal of Physics*, 64(3):225–240, 1996.

[7] J.L. Jain, G. Mohanty, and W. Böhm. *A Course on Queueing Models*. Statistics: A Series of Textbooks and Monographs. CRC Press, 2016.

[8] Sankaran Nampoothiri, Enzo Orlandini, Flavio Seno, and Fulvio Baldovin. Brownian non-gaussian polymer diffusion and queing theory in the mean-field limit. *New Journal of Physics*, 24, 02 2022.